

## Anomalous Linear Dichroism in Bent Chromophores of $\pi$ -conjugated Polymers: Departure from the Franck-Condon Principle

P. Wilhelm,<sup>1</sup> J. Vogelsang,<sup>1</sup> N. Schönfelder,<sup>2</sup> S. Höger,<sup>2</sup> and J. M. Lupton<sup>1,\*</sup>

<sup>1</sup>*Institut für Experimentelle und Angewandte Physik, Universität Regensburg, Universitätsstr. 31, 93053 Regensburg, Germany*

<sup>2</sup>*Kekulé-Institut für Organische Chemie und Biochemie, Universität Bonn, Gerhard-Domagk-Str. 1, 53121 Bonn, Germany*



(Received 10 June 2018; published 8 February 2019)

We examine the influence of bending of  $\pi$ -conjugated chromophores on photoluminescence (PL) by spectrally resolving the depolarization of fluorescence on the single-molecule level. The effect of excited-state mixing mediated by molecular vibrations is manifested in the departure from the usual achromatic linear dichroism of fluorescence, with the polarization anisotropy decreasing in the vibronic progression. Bent chromophores reveal an overall increase in vibronic PL intensity with polarization orthogonal to the molecular long axis. This manifestation of the Renner-Herzberg-Teller (RHT) effect illustrates the breakdown of the Franck-Condon principle in macromolecules used in organic electronics, providing information on the orientation of transition-dipole moments and the origin of spectral broadening. While some of the spectral signatures of the RHT effect appear similar to those of  $H$  aggregation in molecular dimers, discrimination between the two phenomena is straightforward since  $H$  aggregation does not induce anomalous linear dichroism.

DOI: [10.1103/PhysRevLett.122.057402](https://doi.org/10.1103/PhysRevLett.122.057402)

The Franck-Condon principle (FCP)—the approximation that electronic transitions occur much faster than any nuclear rearrangement in a molecule following a change in charge density—is a central assumption in the understanding of macromolecular photophysics. A consequence of the FCP is the decoupling of electronic and nuclear degrees of freedom, which simplifies theoretical descriptions of large  $\pi$ -conjugated systems such as conjugated polymers. The principle implies that the intensity of vibronic optical transitions is proportional to the square of the product of the purely electronic transition-dipole moment (TDM) and the overlap integral of the nuclear wave functions of the initial and final states involved. TDMs of vibronic transitions therefore align with those of purely electronic transitions. In conjugated polymers, the TDM typically extends along the axis of conjugation [1]. The nature of vibronic transitions is crucial to understanding the origin of spectral broadening in materials used to make optoelectronic devices such as solar cells and organic light-emitting diodes (OLEDs) since it determines the effectiveness of light absorption in photovoltaics and color purity in electroluminescence; TDM orientation is critical for light out-coupling in OLEDs. Recently, theoretical studies of the nature of optical transitions based on both tight-binding approximations [2–4] and more detailed quantum molecular dynamics simulations [5] have shown how the FCP can break down with vibrational transitions acquiring oscillator strength due to mixing with higher-lying excited states. Such a breakdown arises from a higher-order perturbative evolution of the nuclear and electronic degrees of freedom, as originally described by Renner, Herzberg, and Teller (RHT) [6–8]. RHT coupling

should become pronounced once the orientation of electronic polarizability, which defines the TDM, deviates from perfect linearity. Such a situation is expected to arise naturally for large  $\pi$ -conjugated molecules making up the film of an optoelectronic device. Molecules in a film will experience strain due to interactions with adjacent molecules, affecting the extension and degree of linearity of their  $\pi$  system in space: The optically active units of the  $\pi$  system, the chromophores, often show signatures of physical bending in the solid state [9,10].

The net result of bending should be a change in the electronic-to-vibronic transition intensity ratio [2,4]. A prediction of the effect of excited-state mixing between different electronic states in bent chromophores is that vibronic transitions acquire a polarization component orthogonal to that of the electronic transitions [2,11]. Such anomalous linear dichroism constitutes a direct spectroscopic observable of the FCP breaking down. However, in an ensemble of molecules such as a film or solution of  $\pi$ -conjugated polymers, the influence of strain on electronic-vibrational coupling will be prohibitively subtle to discriminate deterministically from other effects microscopic molecular structure has on optical spectra [12]: Besides static intersite disorder, energy transfer occurs between different sites, averaging out spectroscopic observables. Here, we probe the predictions of the effect of chromophore bending on the ratio of electronic to vibronic transition intensities [2] using templated molecular models of bent chromophores. Single-molecule spectroscopy shows that vibronic transitions exhibit stronger depolarization than electronic transitions due to their off-axis TDM.

Figure 1 summarizes the elementary process of PL of a chromophore in the framework of the Frenkel-Holstein exciton [2]. The Hamiltonian consists of three parts describing the exciton, nuclear vibrations, and the coupling between exciton and vibrations. As detailed by Barford and Marcus [2], the electronic TDM can be expanded in a Taylor series around a nuclear equilibrium configuration, where the zeroth-order term constitutes the FCP and the first-order term describes the RHT effect. Transition rates can then be computed by applying perturbation theory to the Frenkel-Holstein Hamiltonian. Figure 1(a) contrasts the cases of straight and bent chromophores, which are made up of individual monomer units with a microscopic TDM (small black arrows). We consider the overall TDM arising in the electronic (0-0) and vibronic (0-1) optical transition, indicated by green and orange arrows. The simplest exciton

wave function, a superposition of microscopic dipole oscillations in and out of phase, is sketched for the first ( $k = 0$ ) and second ( $k = 1$ ) excited states for a straight segment (left). For  $k = 0$ , the overall TDM of both electronic and vibronic transitions lies on the  $x$  axis, along the direction of conjugation. For  $k = 1$ , the microscopic TDMs cancel out. The situation differs for a bent chromophore. The TDM of the electronic transition decreases with bending for  $k = 0$ , leading to an increase of the photoluminescence (PL) lifetime ( $\tau_{\text{PL}}$ ) and a reduction of the PL quantum yield ( $QY$ ) of the chromophore, assuming non-radiative decay channels are present. The TDM of  $k = 1$  is now finite and oriented in the  $y$  direction. The fundamental  $k = 0$  mode mixes with the  $k = 1$  mode through vibrational perturbation since the vibronic states of each electronic mode share the same vibrational quantum [2]. This mixing is irrelevant in the straight chromophore but significant in the bent system: Vibronic optical transitions acquire a polarization component due to an orientation of the effective TDM along the  $y$  axis, which compensates for the decrease of vibronic TDM along the  $x$  axis [4]. The ratio between electronic and vibronic peaks ( $I_{0-0}/I_{\text{vib}}$ ) decreases from a straight to a bent chromophore. With these inter-related changes—increasing  $\tau_{\text{PL}}$ , and decreasing  $QY$  and  $I_{0-0}/I_{\text{vib}}$  ratio—it seems feasible to assess the impact of chromophore bending. Unfortunately, dipole coupling between cofacial chromophores can also give rise to  $H$  aggregation or excimer formation, with similar spectral characteristics [12–15], making verification of the RHT effect in *ensembles* of  $\pi$ -conjugated chromophores virtually impossible.

Anticipated PL spectra as a function of polarization angle  $\alpha$  with respect to the  $x$  axis are sketched in Fig. 1(b). Whereas the straight chromophore will show the same normalized spectrum irrespective of light polarization, with the entire luminescence being suppressed in the polarization plane orthogonal to the  $x$  axis ( $90^\circ$ ), the bent chromophore will give rise to a changing ratio of electronic to vibronic peaks depending on fluorescence polarization. In other words, vibronic transitions in a bent chromophore will show stronger depolarization than the electronic transition, offering a spectroscopic signature of bending and making a differentiation from electronic coupling effects between chromophores ( $H$  aggregation) possible. To probe the effect of chromophore bending on fluorescence, we consider a molecular dimer (2) and tetramer (4) of oligo(phenylene-butadiynylene) linked with bithiophene clamping units [16], shown in Fig. 1(c). These structures have the shape of polygons. By reducing the number of sides of the polygon, the shape of the oligomer chromophores—the sides of the polygons—evolves from straight in the squares 4 to bent in the digons 2. This bending is revealed in scanning-tunneling microscopy images and in a range of fluorescence characteristics such as increased  $\tau_{\text{PL}}$ , decreased  $QY$ , and a decreased  $I_{0-0}/I_{\text{vib}}$  ratio [16]. The correlation of spectra with  $\tau_{\text{PL}}$  of the

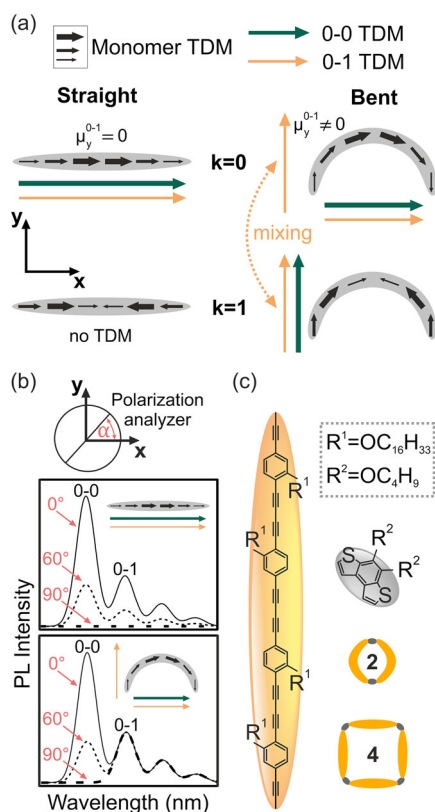


FIG. 1. RHT effect in the fluorescence of bent  $\pi$ -conjugated chromophores, following Ref. [2]. (a) In straight chromophores, the individual monomeric transition-dipole moments (TDMs) add up in the  $x$  direction for the first mode of the excited state ( $k = 0$ ) but cancel out for  $k = 1$ . For a bent chromophore, the  $y$  components of the TDM cancel out for  $k = 0$  but not for  $k = 1$ . The overall TDMs of the 0-0 and the vibronic transitions are indicated in green and orange. Mixing can occur between different excited-state modes by sharing the same vibrational quantum. This mixing gives rise to finite TDMs in the  $y$  direction for the vibronic transitions of the bent chromophore,  $\mu_y^{0-1} \neq 0$ . (b) Resulting polarization anisotropy of the PL spectra of straight and bent chromophores. (c) Molecular polygons used to control chromophore bending, from Ref. [16].

digon **2** can be rationalized within the framework of the FCP. Here, we introduce the technique of single-molecule, spectrally resolved, linear dichroism to reveal a *departure* from the FCP.

Figure 2 summarizes the experimental approach. Panel (a) shows a typical single-molecule PL spectrum of **2**, dispersed in a thin film of poly(methyl-methacrylate), with clearly resolved 0-0 and vibronic peaks. Since single molecules of **2** typically photobleach within a few seconds, we cannot record spectra for all molecules under consideration. Instead, to separate the 0-0 from the vibronic PL intensity, we pass the light through a dichroic mirror, the transmission of which is given in Fig. 2(a) in black. Details of the measurement and background correction procedure are discussed in the Supplemental Material [17]. Besides measuring  $\tau_{\text{PL}}$ , we also record a metric of the fluorescence polarization anisotropy in emission, the modulation depth of the spectrally separated 0-0 and vibronic fluorescence passing a rotating analyzer as sketched in Fig. 2(b). The data in Fig. 2(b) show the cosine-squared modulation of the spectrally resolved PL intensity with time until the molecule bleaches at 0.48 s. The intensity modulations are averaged for each angle of the analyzer and plotted in panel (c) for the 0-0 and vibronic PL contributions. The modulation depth of single-molecule fluorescence  $M_{\text{em}}$  is defined by the difference-to-sum ratio of maximal and minimal PL intensity,  $M_{\text{em}} = (I_{\text{max}} - I_{\text{min}})/(I_{\text{max}} + I_{\text{min}})$

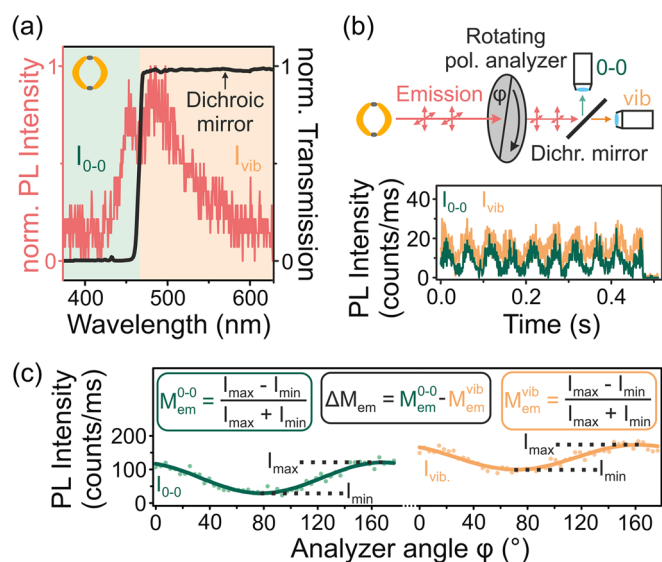


FIG. 2. Probing the RHT effect in single bent chromophores. (a) PL spectrum of a single digon-shaped molecule. The transmission of the dichroic mirror separating the 0-0 and vibronic transitions is given in black. (b) By rotating a polarization analyzer in the emission path, the modulation depth  $M_{\text{em}}$  of the two PL transitions is determined, a measure of the fluorescence polarization anisotropy. The molecule photobleaches after 0.48 s. (c) Summing the PL intensity modulations for each angle of the analyzer gives minimal and maximal PL intensity values, which determined  $M_{\text{em}}$  for the electronic and vibronic PL contributions.

[17,22]. In the example in Fig. 2(c), the electronic transition exhibits stronger modulation than the vibronic, i.e.,  $M_{\text{em}}^{0-0} > M_{\text{em}}^{\text{vib}}$ . We note that because of the scatter of single-molecule spectra, the fixed dichroic mirror will not offer a perfect separation of 0-0 and vibronic PL intensity: Invariably, light from the 0-0 transition will leak into the vibronic detection channel and vice versa. However, this deleterious effect will tend to lower the overall difference between  $M_{\text{em}}^{0-0}$  and  $M_{\text{em}}^{\text{vib}}$  and cannot account for the depolarization of the vibronic transition (i.e.,  $M_{\text{em}}^{0-0} > M_{\text{em}}^{\text{vib}}$ ) [17].

Histograms of the modulation depth of the sum channel of electronic and vibronic PL intensity,  $M_{\text{em}}^{\text{sum}}$ , are shown in Fig. S4 for the two polygon structures **2** and **4** [17]. The tetramer exhibits a broad distribution of modulation depths with an average value of  $M_{\text{em}}^{\text{sum}} = 0.53$ . Low modulation values will arise if the emitting chromophore switches within the molecule. This effect, which arises due to energy transfer between like chromophores, has been identified in combined single-molecule studies and Monte Carlo simulations of exciton localization in bichromophoric systems, where it was shown to give rise to spontaneous fluorescence depolarization [23]. In addition, a small subset of the molecules could conceivably be tilted out of the film plane, lowering the apparent polarization anisotropy, even though, generally, large macrocycle molecules have been found to tend to align within the plane of the film [24]. The dimer **2** reveals a similar distribution around  $M_{\text{em}}^{\text{sum}} = 0.50$ . However, in this measurement it is not clear if low  $M_{\text{em}}$  values arise from molecules exhibiting RHT coupling or if a strain-induced break in the  $\pi$  conjugation of the oligomer gives rise to two effective chromophores with different relative orientations. This latter effect was recently revealed in a detailed study of the photon statistics of bent chromophores: Strong bending can break the  $\pi$  system, giving rise to multichromophoric behavior [20]. Under such conditions, the chromophore responsible for emission may fluctuate within the molecule [23], as in the case of **4**, inducing an effective achromatic depolarization. Very recently, a combined quantum-chemical molecular-dynamics approach to excited-state relaxation has indicated that depolarization of the PL may occur by preferential localization on the bithiophene clamp units [25].

Signatures of RHT coupling are revealed by considering the *difference* between electronic and vibronic PL modulation depths,  $\Delta M_{\text{em}} = M_{\text{em}}^{0-0} - M_{\text{em}}^{\text{vib}}$ . Averaging over 161 (221) single molecules of **4** (**2**), we find  $\Delta M_{\text{em}} = 0.003 \pm 0.007$  for the straight chromophores of **4** and  $\Delta M_{\text{em}} = 0.034 \pm 0.007$  for the bent units of **2** [26]. This difference points to an additional depolarization in the vibronic progression of the fluorescence of the bent units which is not present in straight chromophores. The characteristics of chromophore bending in the dimer are quite heterogeneous as seen by the scatter of spectroscopic observables: There are molecules with a short  $\tau_{\text{PL}}$  and high  $I_{0-0}/I_{\text{vib}}$

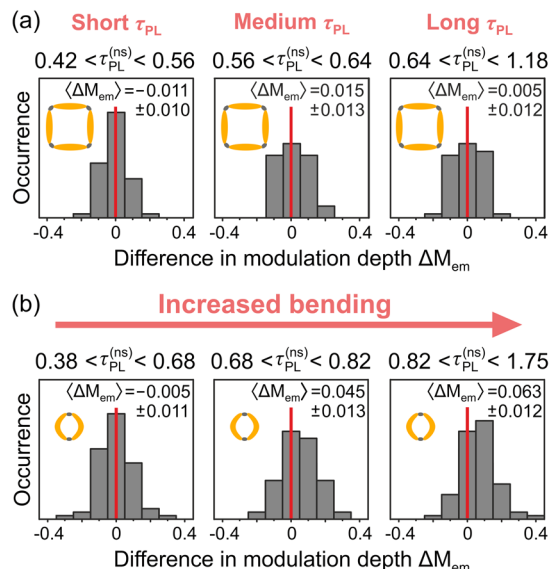


FIG. 3. Vibronically enhanced fluorescence depolarization in single molecules. The difference in polarization modulation depth  $M_{em}$  in PL is considered between the 0-0 and the vibronic transitions,  $M_{em} = M_{em}^{0-0} - M_{em}^{vib}$  for the tetramer **4** (a) and the dimer **2** (b). The molecules are grouped by their fluorescence lifetime  $\tau_{PL}$ , which provides a metric of the TDM and therefore of the degree of chromophore bending.

ratio as well as molecules with a high  $\tau_{PL}$  and low  $I_{0-0}/I_{vib}$  ratio [16]. Since  $\tau_{PL}$  is primarily an indicator of TDM magnitude, which is lowered by bending, a stronger signature of fluorescence depolarization is expected in subgroups of molecules with long  $\tau_{PL}$  and hence stronger bending. We group the molecules by  $\tau_{PL}$  into three sets as stated in Fig. 3 and plot  $\Delta M_{em}$  distributions. No systematic variation of  $\Delta M_{em}$  with  $\tau_{PL}$  occurs for the straight chromophores of **4**, with the average  $\Delta M_{em} \approx 0$ . However, whereas nominally bent chromophores of **2** with the shortest  $\tau_{PL}$  also show no clear deviation of  $\Delta M_{em}$  from zero, implying that the chromophores are not strongly bent, for longer  $\tau_{PL}$  a significant bias is found with  $\Delta M_{em} = 0.063 \pm 0.011$  for the molecules with the longest PL lifetimes and the strongest degree of bending. We conclude that the more pronounced chromophore bending, the stronger the fluorescence depolarization in the vibronic progression of PL. The data also demonstrate conformational variability, which is characteristic of any extended  $\pi$  system embedded in a solid-state environment—even when set in a macrocyclic template. As discussed in the Supplemental Material [17], this spectroscopic approach allows for a distinction between the effect of bending and interchromophoric coupling in cofacial dimers, i.e.,  $H$  aggregation [17]. The two mechanisms show similar effects with regard to the  $I_{0-0}/I_{vib}$  ratio, but no anomalous linear dichroism is observed under  $H$  aggregation, neither in ensemble fluorescence (Fig. S7) nor in single molecules (Fig. S8) [17]. A detailed discussion of the distribution of

$\Delta M_{em}$  values is given in Sec. IV of the Supplemental Material [17]. Finally, we note that signatures of the RHT effect can also be identified in a time-resolved ensemble solution PL of **2** as a wavelength-dependent fluorescence polarization anisotropy  $r(\lambda)$  [17]. The assignment of this anomalous linear dichroism to RHT coupling is, however, only possible having identified the mechanism on the single-molecule level. Only the symmetric dimer **2** reveals these signatures of RHT coupling in the ensemble; in smaller trimers and tetramers with stronger chromophore bending (Figs. S5 and S6),  $r(\lambda)$  is flat (Fig. S7) although on the single-molecule level  $\langle \Delta M_{em} \rangle \neq 0$  (Fig. S8) [17].

While we cannot probe bent chromophores in  $\pi$ -conjugated polymers directly, we argue that bent units and the resulting RHT effect will play a crucial role in determining the PL characteristics in polymer thin films. Bent chromophores have been inferred in polymer ensembles by means of ultrafast fluorescence depolarization spectroscopy, the results of which are hard to reconcile with conventional Förster-type energy transfer between extended units [27–29]. Intuitively, following the particle-in-a-box picture of a chromophore, one may expect that bending should give rise to a shift of the transition energy to shorter wavelengths. As Fig. S2(a) shows, however, it is actually the lowest-energy chromophores which are most bent, implying that energy transfer in thin-film ensembles will also lead to preferential population of these sites. The situation of the oligo(phenylene-butadiynyls) used here is analogous to the case of poly(phenylenevinylene) (PPV), where chromophore bending leads to a strong redshift, spectral broadening, and a loss of vibronic resolution of the PL spectrum [9,30]. In thin films, the PL is dominated by these bent chromophores [30]. In contrast, in dilute frozen solutions of well-solvated PPV chains, where force-induced bending of the chromophores is minimal and interchromophoric energy transfer is less prevalent, higher-energy narrow spectral features with well-resolved vibronic progressions are observed [31].

Naturally, the question arises beyond what degree of bending RHT coupling breaks down so that nonvertical electronic transitions emerge due to conical intersections of excited-state surfaces [32]. Such transitions are often characteristic of photoisomerization processes but are not generally considered in the context of  $\pi$ -conjugated macromolecules used in organic electronics. With the strong chromophore bending that can arise in conjugated polymers, directly visualized as hairpins in scanning-tunneling microscopy [33], ultimately, a complete decoupling between electronic modes and nuclear degrees of freedom may arise. Such decoupling would result in fully nonadiabatic electronic transitions. Since electron-vibrational coupling dynamics occur on timescales of molecular vibrations [34,35], it is encouraging that the impact of these dynamics can be discerned by fluorescence on much longer timescales and, as demonstrated here, even in static single-molecule

measurements. We conclude that single-molecule spectroscopy can, in principle, be used to probe molecular dynamics on timescales much shorter than those of the actual experiment. In contrast to ensemble ultrafast spectroscopies, intermolecular conformational heterogeneities can be resolved in order to parametrize microscopic computational models [35].

The authors thank M. Marcus and W. Barford for inspiring discussions and are indebted to the German Science Foundation for funding through Collaborative Grant No. 319559986.

\*Corresponding author.

john.lupton@ur.de

- [1] T. W. Hagler, K. Pakbaz, and A. J. Heeger, *Phys. Rev. B* **49**, 10968 (1994).
- [2] W. Barford and M. Marcus, *J. Chem. Phys.* **145**, 124111 (2016).
- [3] M. Marcus, J. Coonjobeeharry, and W. Barford, *J. Chem. Phys.* **144**, 154102 (2016).
- [4] N. J. Hestand and F. C. Spano, *J. Phys. Chem. B* **118**, 8352 (2014).
- [5] L. Adamska, I. Nayyar, H. Chen, A. K. Swan, N. Oldani, S. Fernandez-Alberti, M. R. Golder, R. Jasti, S. K. Doorn, and S. Tretiak, *Nano Lett.* **14**, 6539 (2014).
- [6] G. Herzberg and E. Teller, *Z. Phys. Chem., Abt. B* **21**, 410 (1933).
- [7] R. Renner, *Z. Phys.* **92**, 172 (1934).
- [8] I. B. Bersuker, *Chem. Rev.* **101**, 1067 (2001).
- [9] K. Becker, E. Da Como, J. Feldmann, F. Scheliga, E. Thorn Csányi, S. Tretiak, and J. M. Lupton, *J. Phys. Chem. B* **112**, 4859 (2008).
- [10] T. Adachi, J. Vogelsang, and J. M. Lupton, *J. Phys. Chem. Lett.* **5**, 2165 (2014).
- [11] J. K. Sprafke *et al.*, *J. Am. Chem. Soc.* **133**, 17262 (2011).
- [12] B. J. Schwartz, *Annu. Rev. Phys. Chem.* **54**, 141 (2003).
- [13] F. C. Spano and C. Silva, *Annu. Rev. Phys. Chem.* **65**, 477 (2014).
- [14] S. Liu, D. Schmitz, S.-S. Jester, N. J. Borys, S. Höger, and J. M. Lupton, *J. Phys. Chem. B* **117**, 4197 (2013).
- [15] T. Stangl, P. Wilhelm, D. Schmitz, K. Remmerssen, S. Henzel, S.-S. Jester, S. Höger, J. Vogelsang, and J. M. Lupton, *J. Phys. Chem. Lett.* **6**, 1321 (2015).
- [16] P. Wilhelm, J. Vogelsang, G. Poluektov, N. Schönfelder, T. J. Keller, S. S. Jester, S. Höger, and J. M. Lupton, *Angew. Chem., Int. Ed. Engl.* **56**, 1234 (2017).
- [17] See Supplemental Material at <http://link.aps.org/supplemental/10.1103/PhysRevLett.122.057402> for details on measurement techniques and additional ensemble and single-molecule data sets, which includes Refs. [18–21].
- [18] J. R. Lakowicz, *Principles of Fluorescence Spectroscopy*, 3rd ed. (Kluwer Academic/Plenum, New York, 2006), p. 353.
- [19] S.-S. Jester, E. Sigmund, and S. Höger, *J. Am. Chem. Soc.* **133**, 11062 (2011).
- [20] K. Becker, M. Fritzsche, S. Höger, and J. M. Lupton, *J. Phys. Chem. B* **112**, 4849 (2008).
- [21] P. Wilhelm, J. Schedlbauer, F. Hinderer, D. Hennen, S. Höger, J. Vogelsang, and J. M. Lupton, *Proc. Natl. Acad. Sci. U.S.A.* **115**, E3626 (2018).
- [22] P. F. Barbara, A. J. Gesquiere, S.-J. Park, and Y. J. Lee, *Acc. Chem. Res.* **38**, 602 (2005).
- [23] T. Stangl, S. Bange, D. Schmitz, D. Würsch, S. Höger, J. Vogelsang, and J. M. Lupton, *J. Am. Chem. Soc.* **135**, 78 (2013).
- [24] D. Würsch, F. J. Hofmann, T. Eder, A. V. Aggarwal, A. Idelson, S. Höger, J. M. Lupton, and J. Vogelsang, *J. Phys. Chem. Lett.* **7**, 4451 (2016).
- [25] D. Ondarse-Alvarez, T. Nelson, J. M. Lupton, S. Tretiak, and S. Fernandez-Alberti, *J. Phys. Chem. Lett.* **9**, 7123 (2018).
- [26] The error stated is the standard error of the mean.
- [27] M. M.-L. Grage, Y. Zaushitsyn, A. Yartsev, M. Chachisvilis, V. Sundström, and T. Pullerits, *Phys. Rev. B* **67**, 205207 (2003).
- [28] A. Ruseckas, P. Wood, I. D. W. Samuel, G. R. Webster, W. J. Mitchell, P. L. Burn, and V. Sundström, *Phys. Rev. B* **72**, 115214 (2005).
- [29] W. J. D. Beenken and T. Pullerits, *J. Phys. Chem. B* **108**, 6164 (2004).
- [30] B. Schwartz, *Nat. Mater.* **7**, 427 (2008).
- [31] J. D. Milward, M. Marcus, A. Köhler, and W. Barford, *J. Chem. Phys.* **149**, 044903 (2018).
- [32] S. Nanbu, T. Ishida, and H. Nakamura, *Chem. Sci.* **1**, 663 (2010).
- [33] E. Mena-Osteritz *et al.*, *Angew. Chem., Int. Ed. Engl.* **39**, 2679 (2000).
- [34] J. Clark, T. Nelson, S. Tretiak, G. Cirmi, and G. Lanzani, *Nat. Phys.* **8**, 225 (2012).
- [35] S. Tretiak, A. Saxena, R. L. Martin, and A. R. Bishop, *Phys. Rev. Lett.* **89**, 097402 (2002).